 doi:10.20944/preprints202208.0446.v1

Brief Report

Intramolecular Isotope Analysis enables Multivariate Climate Reconstructions

Thomas Wieloch[1,*], Jun Yu[2], Jürgen Schleucher[3] and Totte Niittylä[1]

[1] Department of Forest Genetics and Plant Physiology, Swedish University of Agricultural Sciences, Umeå Plant Science Centre, 90183 Umeå, Sweden
[2] Department of Mathematics and Mathematical Statistics, Umeå University, 90187 Umeå, Sweden
[3] Department of Medical Biochemistry and Biophysics, Umeå University, 90187 Umeå, Sweden
*Corresponding author: thomas.wieloch@umu.se

Abstract: Paleoclimate information is key to understanding the climate system and predicting future climate. Currently, stable isotope analysis of whole molecules in tree rings is among the most advanced paleoclimate tools. Still, it only enables reconstructions of one climate parameter at a time (univariate climate reconstruction), a fundamental limitation. Here, we investigated whether this limitation can be overcome by analysing isotope variability at the level of intramolecular carbon positions in tree-ring glucose. We found that drought governs isotope variability at glucose C-1 to C-3, whereas radiation governs isotope variability at glucose C-5 to C-6. These isotope-climate relationships are statistically and mechanistically robust. According to cross-validation analysis, they can be reconstructed with high accuracy and precision. Thus, intramolecular isotope analysis enables multivariate climate reconstructions (proof of concept).

Keywords: climate reconstruction; nuclear magnetic resonance spectroscopy; paleoclimate information; stable isotope analysis; tree rings

1. Introduction

Information about paleoclimates (i.e., climates for which there are no direct measurements) is key to understanding the climate system and predicting future climate (1). Moreover, paleoclimate information can put into perspective historical and prehistorical events such as the collapse of ancient societies (2) and mass extinctions (3). Analysis of carbon stable isotope composition (^{12}C, ^{13}C) across tree-ring series is among the most advanced tools for reconstructing terrestrial climate conditions. Since the mid-1950s, measurements have been performed on whole-tissue or whole-molecule samples yielding a single isotope series per tree-ring series (Fig. 1A, 4). Consequently, conventional carbon isotope analysis enables the reconstruction of only one climate parameter at a time (univariate climate reconstruction), a fundamental limitation. Today, nuclear magnetic resonance spectroscopy allows carbon isotope measurements at intramolecular atom positions, thus supplying data at a higher resolution (Fig. 1A). Recently, we reported intramolecular $^{13}C/^{12}C$ ratios in glucose extracted across an annually resolved tree-ring series of *Pinus nigra* covering the period 1961 to 1995 (n = 6*31, four years missing) (5). Since glucose has six carbon atoms (Fig. 1A), the dataset comprises six $^{13}C/^{12}C$ series. We expressed these data in terms of intramolecular ^{13}C discrimination, a measure of $^{13}C/^{12}C$ variability caused by plant physiological processes ($\Delta i'$, i denotes glucose carbon positions) (5, 6). Previous statistical analyses revealed that the dataset conveys information about several physiological processes with differential responses to environmental cues (5, 7–9). Here, we test whether the dataset can be used to simultaneously reconstruct multiple climate parameters. Augusti *et al.* (10) already proposed multivariate climate reconstruction is feasible by intramolecular hydrogen isotope analysis. However, proof of concept has not yet been reported for any chemical element.

Preprints (www.preprints.org) | NOT PEER-REVIEWED | Posted: 26 August 2022 doi:10.20944/preprints202208.0446.v1

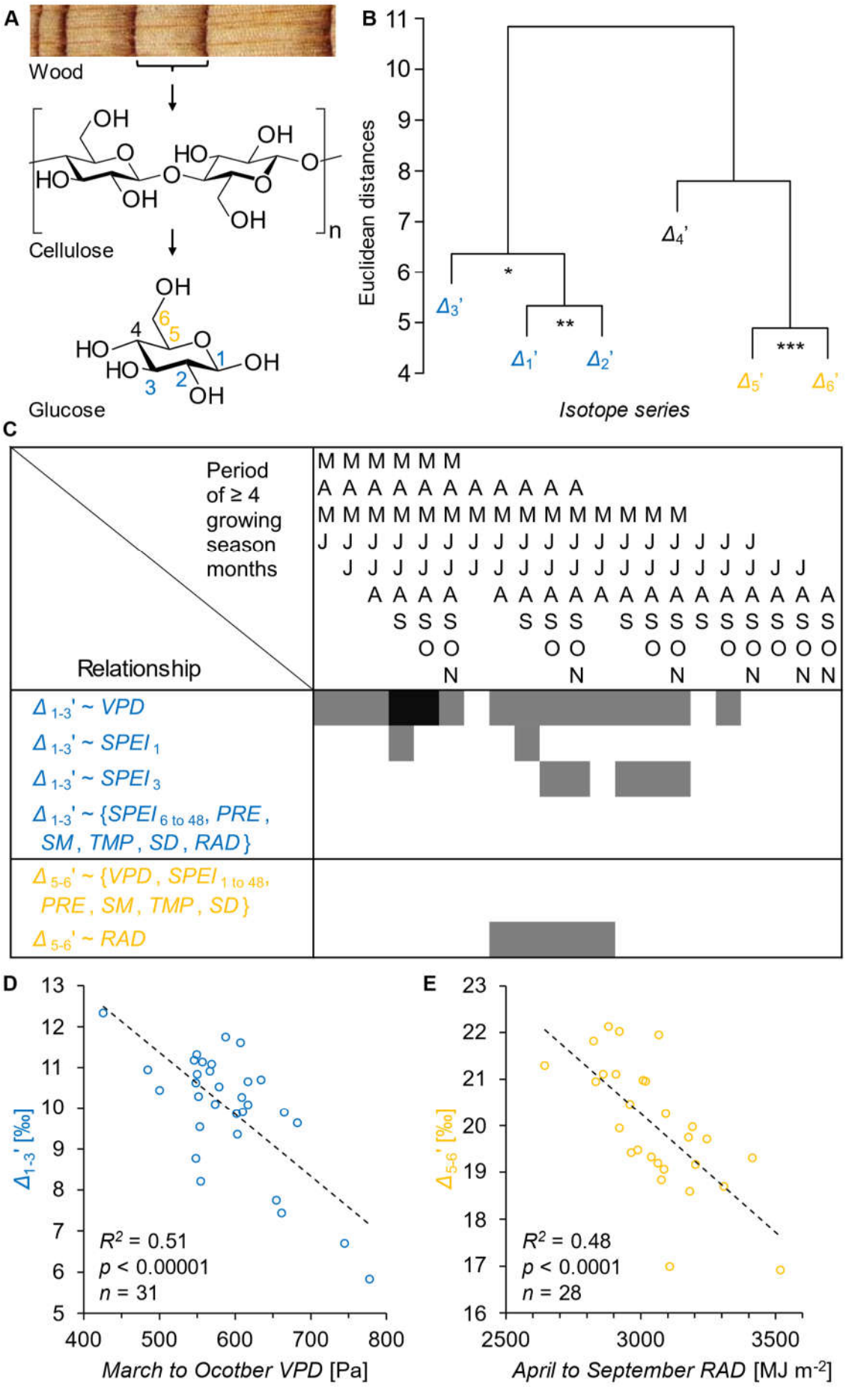

 doi:10.20944/preprints202208.0446.v1

Figure 1. Drought and radiation govern carbon isotope discrimination at glucose C-1 to C-3 and C-5 to C-6, respectively. (A) Levels of resolution of stable carbon isotope analysis: whole plant materials, whole molecules, intramolecular carbon positions. **(B)** Hierarchical clustering of Δ_i' series. Significance of series correlation: *, $p \leq 0.05$; **, $p \leq 0.01$; ***, $p \leq 0.001$. Modified figure from Wieloch *et al.* (5). **(C)** Significance of correlation between isotope and climate series: black, $p \leq 0.00001$; grey, $p \leq 0.0001$ ($p > 0.0001$ not shown). Climate data averaged for all ≥ 4-month periods of the growing season. Months abbreviated by their initial letters. **(D)** Relationship between $\Delta_{1\text{-}3}'$ and *March to October VPD*. **(E)** Relationship between $\Delta_{5\text{-}6}'$ and *April to September RAD*. Dashed lines, linear regression models. Δ_i' denotes intramolecular ^{13}C discrimination in glucose extracted across an annually resolved *Pinus nigra* tree-ring series (1961-1995). $\Delta_{1\text{-}3}'$ and $\Delta_{5\text{-}6}'$ denote average discriminations of glucose C-1 to C-3 and C-5 to C-6, respectively. Abbreviations: *PRE*, precipitation; *RAD*, global radiation; *SD*, sunshine duration; *SM*, soil moisture; $SPEI_i$, standardised precipitation-evapotranspiration index of different periods (i = 1, 3, 6, 8, 12, 16, 24, 36, 48 months); *TMP*, air temperature; *VPD*, air vapour pressure deficit.

2. Results

Hierarchical cluster analysis groups Δ_i' series according to co-variability. Both hierarchical cluster analysis and correlation analysis show that average ^{13}C discrimination of glucose C-1 to C-3 ($\Delta_{1\text{-}3}'$) is independent of average ^{13}C discrimination of glucose C-5 to C-6 ($\Delta_{5\text{-}6}'$, Fig. 1B, $r = 0.12$, $p > 0.5$, $n = 31$). Thus, $\Delta_{1\text{-}3}'$ and $\Delta_{5\text{-}6}'$ convey information about different physiological processes (9). To investigate which climate parameters exert predominant control over these processes and may thus be reconstructed at high quality, we correlated $\Delta_{1\text{-}3}'$ and $\Delta_{5\text{-}6}'$ with air temperature (*TMP*), air vapour pressure deficit (*VPD*), global radiation (*RAD*), precipitation (*PRE*), soil moisture (*SM*), sunshine duration (*SD*), and the standardised precipitation-evapotranspiration index of different periods ($SPEI_i$, i = 1, 3, 6, 8, 12, 16, 24, 36, 48 months). The *SPEI* is a multi-scalar drought index where short timescales approximate soil moisture variability while long timescales approximate groundwater variability. Correlation analysis considered climate conditions of all ≥ 4-month periods of the growing season (March to November, 5). We found $\Delta_{1\text{-}3}'$ correlates most significantly with *VPD* whereas $\Delta_{5\text{-}6}'$ correlates most significantly with *RAD* (Fig. 1C; $\Delta_{1\text{-}3}'$ ~ *VPD*: $p < 0.00001$, $n = 31$; $\Delta_{5\text{-}6}'$ ~ *RAD*: $p < 0.0001$, $n = 28$; Datasets 1-2). Among all periods tested, *March to October VPD* and *April to September RAD* explain most of the variability in $\Delta_{1\text{-}3}'$ (51%) and $\Delta_{5\text{-}6}'$ (48%), respectively (Figs. 1D-E; $\Delta_{1\text{-}3}' = -0.01515VPD + 18.95$; $\Delta_{5\text{-}6}' = -0.005075RAD + 35.48$). Of the total variance in $\Delta_{1\text{-}3}'$ and $\Delta_{5\text{-}6}'$, 88% and 75% are explainable by modelling, while 12% and 25% are due to measurement error, respectively. Hence, *March to October VPD* and *April to September RAD* respectively explain 58% and 64% of the explainable variance in $\Delta_{1\text{-}3}'$ and $\Delta_{5\text{-}6}'$ and are thus promising candidates for climate reconstruction. To test how well these parameters can be reconstructed, we split $\Delta_{1\text{-}3}'$ and $\Delta_{5\text{-}6}'$ into two sub-datasets of similar size. Data pertaining to odd years were used to train isotope-climate models (Figs. 2A-B). Subsequently, these models were used to reconstruct *March to October VPD* and *April to September RAD* of even years. Regression analyses show significant association between reconstructed and observed data where intercepts and slopes are not significantly different from zero and unity, respectively (Figs. 2C-D; *March to October VPD'* ~ *March to October VPD*: $R^2 = 0.46$, $p < 0.01$, $n = 15$, *intercept* = 149 ± 314 95% CI, *slope* = 0.815 ± 0.526 95% CI; *April to September RAD'* ~ *April to September RAD*: $R^2 = 0.56$, $p < 0.01$, $n = 14$, *intercept* = -520 ± 2034 95% CI, *slope* = 1.19 ± 0.66 95% CI; reconstructed data marked by prime). Hence, both climate parameters can be reconstructed with significant accuracy and precision. Results from this two-fold cross-validation analysis are corroborated by results from ten-fold cross-validation analysis ($\Delta_{1\text{-}3}'$ ~ *March to October VPD*: $Q^2 = 0.46$, $p < 0.0001$, $n = 31$; $\Delta_{5\text{-}6}'$ ~ *April to September RAD*: $Q^2 = 0.37$, $p < 0.001$, $n = 28$).

Preprints (www.preprints.org) | NOT PEER-REVIEWED | Posted: 26 August 2022 doi:10.20944/preprints202208.0446.v1

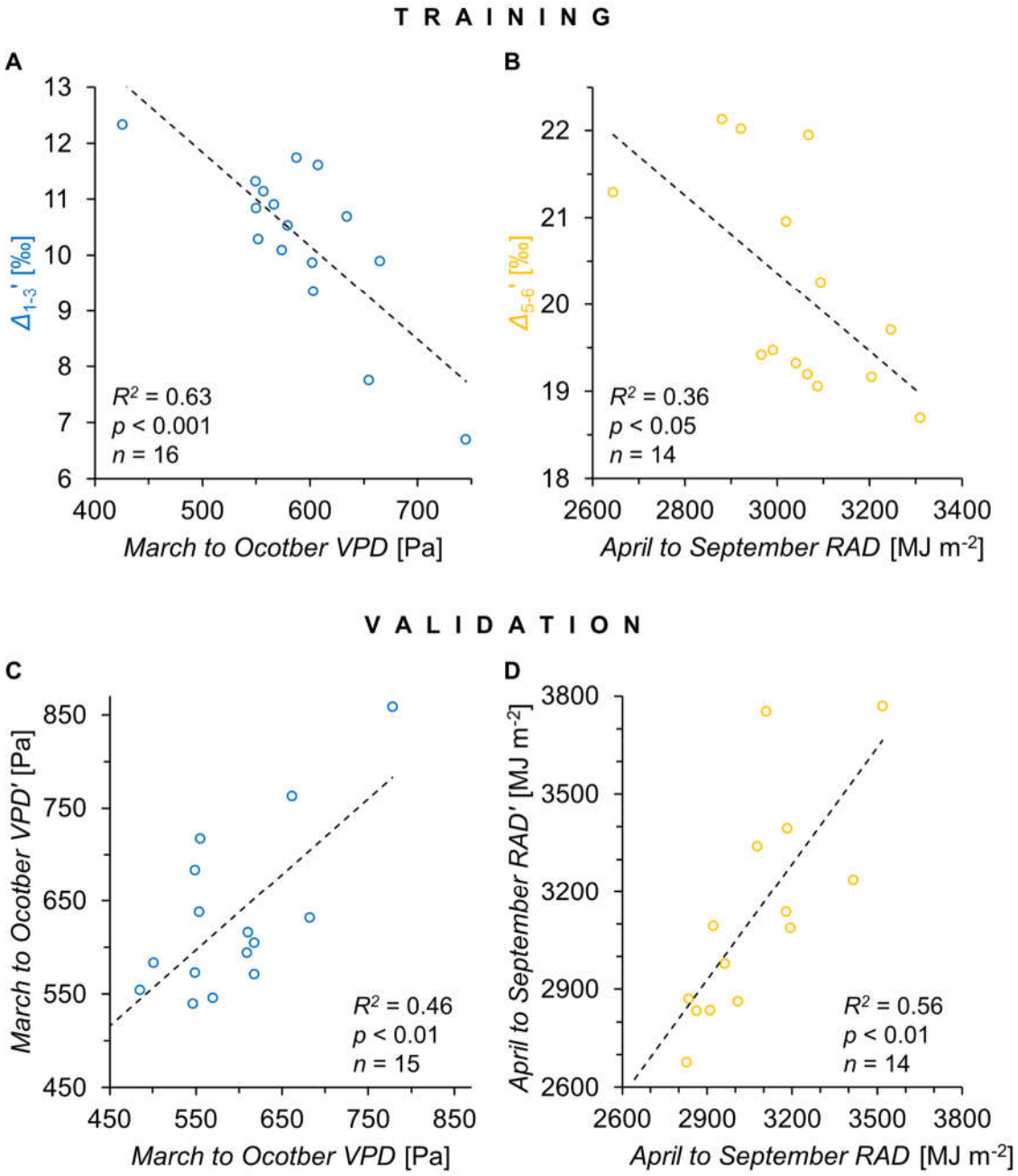

Figure 2. Intramolecular carbon isotope analysis enables multivariate climate reconstructions. **(A-B)** Training of isotope-climate models with the data of odd years ($\Delta_{1\text{-}3}$' ~ *March to October VPD*, $\Delta_{5\text{-}6}$' ~ *April to September RAD*). Trained models were used to reconstruct the climate of even years. **(C-D)** Validation of isotope-climate models with the data of even years (*March to October VPD'* ~ *March to October VPD*: *intercept* = 149 ± 314 95% CI, *slope* = 0.815 ± 0.526 95% CI; *April to September RAD'* ~ *April to September RAD*: *intercept* = -520 ± 2034 95% CI, *slope* = 1.19 ± 0.66 95% CI; reconstructed data marked by prime). Dashed lines, linear regression models. $\Delta_{1\text{-}3}$' and $\Delta_{5\text{-}6}$' denote average intramolecular ^{13}C discrimination of glucose C-1 to C-3, and C-5 to C-6, respectively. Glucose was extracted across an annually resolved tree-ring series of *Pinus nigra* (1961-1995). Abbreviations: *RAD*, global radiation; *VPD*, air vapour pressure deficit.

3. Discussion

Isotope variation at glucose C-1 to C-3 is thought to derive from ^{13}C discrimination accompanying air-rubisco CO_2 diffusion and rubisco CO_2 fixation (5). In isohydric species such as *Pinus nigra*, stomata close in response to drought, causing CO_2 reduction around rubisco (11) and decreased diffusion-rubisco ^{13}C discrimination (6). Additionally, drought

is thought to cause decreased ^{13}C discrimination at glucose C-1 and C-2 by a mechanism involving phosphoglucose isomerase (5). Both ecophysiological mechanisms are consistent with the negative relationship between $\Delta_{1\text{-}3}'$ and *VPD* reported here (Fig. 1D). Discrimination at glucose C-5 to C-6 is thought to decrease with the leaf-level consumption of phospho*enol*pyruvate (PEP) by downstream metabolism (9). Several ecophysiological mechanisms may explain the negative relationship between $\Delta_{5\text{-}6}'$ and *RAD* reported here (Fig. 1E). First, *Pinus nigra* is ozone-sensitive (12), and light can stimulate tropospheric ozone formation (13). Ozone activates both PEP carboxylase and enzymes of the shikimate pathway causing increased PEP consumption (14–16). Second, light stimulates fatty acid biosynthesis and thus PEP consumption by pyruvate kinase (17). Third, amino acid concentrations increase with light (18) which may indicate increased PEP consumption by amino acid biosynthesis. In conclusion, the present study reports statistically and mechanistically robust isotope-climate relationships. It shows that intramolecular isotope analysis enables multivariate climate reconstructions (proof of concept) and may thus help to advance our knowledge about past climate conditions and climate system functioning.

4. Materials and Methods

Isotope data have been published previously (5). Climate data were retrieved from public repositories. Comprehensive information about the methods can be found in SI Appendix.

Author Contributions: Conceptualisation: TW, Investigation: TW with input from JY, Visualization: TW, Project administration: TW, Writing – original draft: TW with input from all authors.

Data, Materials, and Software Availability: All study data are included in the article and/or supporting information.

Conflicts of Interest: The authors declare no conflict of interest.

References

1. R. S. Bradley, "Chapter 1 - Paleoclimatic reconstruction" in *Paleoclimatology (Third Edition)*, R. S. Bradley, Ed. (Academic Press, 2015), pp. 1–11.
2. P. B. deMenocal, Cultural responses to climate change during the late Holocene. *Science* **292**, 667–673 (2001).
3. H. Song, *et al.*, Thresholds of temperature change for mass extinctions. *Nat. Commun.* **12**, 4694 (2021).
4. H. Craig, Carbon-13 variations in Sequoia rings and the atmosphere. *Science* **119**, 141–143 (1954).
5. T. Wieloch, *et al.*, Intramolecular ^{13}C analysis of tree rings provides multiple plant ecophysiology signals covering decades. *Sci. Rep.* **8**, 5048 (2018).
6. G. D. Farquhar, J. R. Ehleringer, K. T. Hubick, Carbon isotope discrimination and photosynthesis. *Annu. Rev. Plant Physiol. Plant Mol. Biol.* **40**, 503–537 (1989).
7. T. Wieloch, A cytosolic oxidation–reduction cycle in plant leaves. *J. Exp. Bot.* **72**, 4186–4189 (2021).
8. T. Wieloch, R. A. Werner, J. Schleucher, Carbon flux around leaf-cytosolic glyceraldehyde-3-phosphate dehydrogenase introduces a ^{13}C signal in plant glucose. *J. Exp. Bot.* **72**, 7136–7144 (2021).
9. T. Wieloch, T. D. Sharkey, R. A. Werner, J. Schleucher, Intramolecular carbon isotope signals reflect metabolite allocation in plants. *J. Exp. Bot.* **73**, 2558–2575 (2022).
10. A. Augusti, T. R. Betson, J. Schleucher, Deriving correlated climate and physiological signals from deuterium isotopomers in tree rings. *Chem. Geol.* **252**, 1–8 (2008).
11. N. Sade, A. Gebremedhin, M. Moshelion, Risk-taking plants: anisohydric behavior as a stress-resistance trait. *Plant Signal. Behav.* **7**, 767–770 (2012).
12. A. S. Lefohn, *Surface-level ozone exposures and their effects on vegetation* (CRC Press, 1992).
13. X. Lu, L. Zhang, L. Shen, Meteorology and climate influences on tropospheric ozone: a review of natural sources, chemistry, and transport patterns. *Curr. Pollut. Rep.* **5**, 238–260 (2019).
14. P. Dizengremel, Effects of ozone on the carbon metabolism of forest trees. *Plant Physiol. Biochem.* **39**, 729–742 (2001).
15. I. Janzik, S. Preiskowski, H. Kneifel, Ozone has dramatic effects on the regulation of the prechorismate pathway in tobacco (*Nicotiana tabacum* L. cv. Bel W3). *Planta* **223**, 20–27 (2005).
16. G. A. Betz, *et al.*, Ozone affects shikimate pathway genes and secondary metabolites in saplings of European beech (*Fagus sylvatica* L.) grown under greenhouse conditions. *Trees* **23**, 539–553 (2009).
17. Y. Sasaki, A. Kozaki, M. Hatano, Link between light and fatty acid synthesis: Thioredoxin-linked reductive activation of plastidic acetyl-CoA carboxylase. *Proc. Natl. Acad. Sci. U.S.A.* **94**, 11096–11101 (1997).

 doi:10.20944/preprints202208.0446.v1

18. D. Toldi, *et al.*, Light intensity and spectrum affect metabolism of glutathione and amino acids at transcriptional level. *PLoS ONE* **14**, e0227271 (2019).